Pharmacology Research & Perspectives

ORIGINAL ARTICLE OPEN ACCESS

The TAAR1 Agonist PCC0105004 Regulates Amygdala Synaptic Plasticity to Alleviate Anxiety-Like Behaviors in Rats

Yingtian Zhang[1] | Wei Zhang[1] | Linyao Yu[1] | Yaoqin Shi[1] | Min Xu[1] | Hui Wang[2] | Chunmei Li[1,2] | Jingwei Tian[1,2]

[1]School of Pharmacy, Key Laboratory of Molecular Pharmacology and Drug Evaluation (Yantai University), Ministry of Education, Collaborative Innovation Center of Advanced Drug Delivery System and Biotech Drugs in Universities of Shandong, Yantai University, Yantai, People's Republic of China | [2]State Key Laboratory of Advanced Drug Delivery and Release Systems, Yantai, Shandong, People's Republic of China

Correspondence: Chunmei Li (lichunmei@luye.com) | Jingwei Tian (tianjingwei618@163.com)

Received: 8 November 2024 | **Revised:** 26 December 2024 | **Accepted:** 10 January 2025

Funding: This work was supported by Science and Technology Project of Yantai (No. 2023XDRH008) and Major Basic Research Special Projects of Shandong Provincial, China (ZR2024ZD21).

Keywords: amygdala | anxiety | PCC0105004 | synaptic plasticity | TAAR1

ABSTRACT

Anxiety disorder is a persistent, widespread, and intractable mood disorder, and the available pharmacotherapies have limited efficacy with significant side effects. Trace amine-associated receptor 1 (TAAR1) is an emerging drug target for neuropsychiatric disorders. This study examined the effects and underlying mechanisms of a novel TAAR1 agonist, PCC0105004, in a rat model of CUMS-induced anxiety-like behavior. The elevated zero maze and open field tests test were employed to evaluate the anti–anxiety-like activity of PCC0105004. PCC0105004 dose-dependently attenuated anxiety-like behaviors in rats without affecting spontaneous activity. Morphologically, PCC0104005 decreased the density of dendritic spines in the amygdala. For the mechanistic studies, whole-genome transcriptomic analysis revealed significant differences in the patterns of amygdala gene expression in the CUMS-induced anxiety rat model. These transcriptomic data were further confirmed by using RT-qPCR and western blotting, further revealing alterations associated with genes (*Col1a1, DCN, Ewsr1*) known to regulate synaptic plasticity, and PCC0105004 was able to reverse these changes. These results suggest that PCC0105004 is a promising anxiolytic candidate for pharmacotherapy of anxiety and warrants further examination and development.

1 | Introduction

Anxiety disorders (ADs) form the most common type of mental illness [1]. The World Health Organization (WHO) ranks anxiety disorders as the ninth most health-related cause of disability [2]. In 2019, 87 studies from 44 countries indicated that the global prevalence of this disorder has fluctuated between 0.9% and 28.3% [3]. While psychological and social support plays a crucial role in managing anxiety, medication currently stands as the primary treatment modality. Most anxiety cases are currently treated with serotonin reuptake inhibitors (SSRIs), serotonin noradrenaline reuptake inhibitors (SNRIs), opipramol (TCAs), benzodiazepines, and buspirone [4]. However, current antianxiety medications have insufficient overall efficacy in short-term and long-term treatments [5, 6] and of greater concern is their association with substantial side effects, which include slow onset of therapeutic effect [7], low tolerability [8], GI disturbance [9], sexual dysfunction, and persistent disturbed sleep [10]. Thus, considering the limitations associated with currently available anti-anxiety drugs, there is a need to look for a mechanistically novel with less toxic therapy in anxiety patients. A future atypical antipsychotic target trace amine-associated receptor 1 (TAAR1) may have the potential to serve as a novel anti-anxiety drug target.

This is an open access article under the terms of the Creative Commons Attribution-NonCommercial-NoDerivs License, which permits use and distribution in any medium, provided the original work is properly cited, the use is non-commercial and no modifications or adaptations are made.

© 2025 The Author(s). *Pharmacology Research & Perspectives* published by British Pharmacological Society and American Society for Pharmacology and Experimental Therapeutics and John Wiley & Sons Ltd.

The G-protein-coupled receptor (GPCR) TAAR1 is expressed throughout the mesolimbic monoaminergic system [11], with expression in regions of the brain including the hippocampus and the extended amygdala [12], both of which are closely linked to the neuropathological basis of anxiety [13, 14]. A growing number of studies suggest that TAAR1 serves as a modulator of monoaminergic neurotransmission [15, 16]. TAAR1 agonists, such as the full agonist RO5166017 and partial agonist RO5256390, can inhibit the excitability of 5-HT and dopamine neurons [17–20]. Endogenous ligands of TAAR1 and selective agonists of this receptor also present with anxiolytic-like activity in published behavioral studies [21]. Both the TAAR1 full agonist RO5166017 and partial agonist RO5203648, for instance, could block stress-induced hyperthermia, indicating anxiolytic properties of TAAR1 agonists [18, 19], and chronic treatment with RO5166017 completely prevented post-traumatic stress disorder (PTSD) [22]. However, chronic treatment of the TAAR1 partial agonist RO5263397 had no effect on chronic stress-induced anxiety-like behaviors [23] or partially attenuated PTSD [22]. Ulotaront (SEP-363856) is one of the selective TAAR1 full agonists that entered randomized controlled phase II/III clinical trials (NCT05729373) for the treatment of schizophrenia, which is currently under clinical evaluation for managing generalized anxiety disorder [24].

While processing anxiety-related information involves a wide range of brain regions, a key structure in this network is the amygdala [25, 26]. The dysfunctional neural plasticity in the amygdala has long been proposed as the vital cause for the progression of anxiety [27–29]. Neurons in the amygdala are highly sensitive to stress and anxiety-inducing stimuli, undergoing significant remodeling following stressor exposure [30]. A number of literatures showed that activation of anxiety-like behaviors triggers dendritic spines that were reduced [31–34], and their genes were also downregulated [35].

PCC0105004 4 [(*S*)-4,7,8,9,10,10a-hexahydro-5*H*-thieno [2′,3′:3,4] pyrido [1,2-a] pyrazine] is a novel TAAR1 full agonist with high efficacy and good potency (EC50 value of 0.06182 μM, E_{max} value of 92.9%) in vitro assessments. Pharmacokinetic evaluation shows that the highest concentrations of PCC0105004 in plasma and brain are observed at 0.25–1 h after drug administration in rats, with the brain/plasma ratio ranging from 8.45 to 4.22, demonstrating a favorable pharmacokinetic profile. These results support the evaluation of PCC0105004 as a TAAR1 full agonist for subsequent experiments [36].

In this study, a chronic unpredictable mild stress (CUMS)-induced model of anxiety was used to evaluate the anxiolytic-like activity of PCC0105004 and to clarify the neurobiological mechanisms through which it exerts its beneficial effects.

2 | Materials and Methods

2.1 | Animals

Adult Sprague–Dawley (SD) rats (males, 180–200 g, 6–7 weeks) were obtained from Beijing Vital River Laboratory Animal Technology Co Ltd. (Beijing, China) and maintained in a certified animal facility under controlled conditions (21°C–23°C, 40%–60% humidity, 12 h light/dark cycle) with ad libitum food and water access. Behavioral testing was only performed after allowing these rats to acclimate to the testing environment for 7 days. Investigators remained blinded to experimental treatment during behavioral testing, and all behavioral tests were performed between the hours of 8:00 and 14:00. The experimental approaches used in this study were implemented as per the ARRIVE guidelines (Kilkenny, Browne, Cuthill, Emerson &Altman, 2010), and the Laboratory Animals Care and Use Committee of Yantai University (Yantai, China) provided approval for all animal studies described herein (registration number: YTU20230110).

2.2 | Drugs and Chemicals

PCC0105004 ($C_{10}H_{14}N_2S$, Figure 1) with 95% purity was obtained from WuXi AppTec (Tianjin, China). Powdered diazepam (DZP) was purchased from Shandong Xinyi Pharmaceutical Co. Ltd. (Shandong, China). PCC0105004 was dissolved in normal saline (0.9% NaCl, Sal), while DZP [37] was resuspended with 0.5% sodium carboxymethyl cellulose (CMC-Na). Drug solutions were prepared fresh prior to use.

2.3 | CUMS Modeling

The CUMS protocol was used to establish a rat model of anxiety [38, 39]. Briefly, all rats (experimental rats) other than those in the control group were subjected to mild unpredictable stress treatment for 21 days, with the stressors used for this approach including restraint (4 h), cage tilting (45° for 24 h), wet bedding (24 h), deprivation of food and/or water (24 h), tail nip (1 cm from the end of the tail for 3 min), swimming in cold water (4°C for 3 min), and light inversion (24 h). For such modeling, rats were individually housed and subjected to different stressors per day administered in a random order. The control group was kept with 5 rats per cage without any stimulation.

2.4 | Experimental Approach

2.4.1 | Experiment 1: Effect of PCC0105004 on the Locomotor Activity in Rats

We evaluated the potential sedative effects of PCC0105004 both in normal rats. After 7 days of acclimation to the housing environment, rats were randomized into seven groups ($n = 10$/

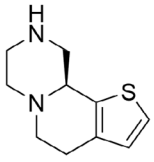

(*S*)-4,7,8,9,10,10a-hexahydro-5*H*-thieno[2',3':3,4]pyrido[1,2-*a*]pyrazine

FIGURE 1 | The chemical structure of PCC0105004, (*S*)-4,7,8,9,10,10a-hexahydro-5*H*-thieno [2′,3′:3,4] pyrido [1,2-a] pyrazine.

group), including a control group, a vehicle group (Sal), and five PCC0105004 treatment groups (1, 2, 3, 4, or 5 mg/kg). At 30 min following the intragastric (ig) administration of the appropriate treatments, rat locomotor activity was analyzed in an open field test (OFT) chamber.

2.4.2 | Experiment 2: Effects of PCC0105004 in the Elevated Zero Maze (EZM) Test in Rats

A more accurate and effective dose was selected for follow-up experiments. As a positive group, i.g. of 2 mg/kg DZP was used based on prior reports [37, 40, 41]. After 7 days of acclimation to the housing environment, rats were randomized into eight groups ($n = 10$/group), including control, vehicle (Sal), DZP (2 mg/kg), and PCC0105004 (0.5, 0.75, 1, 2, and 3 mg/kg) groups. At 30 min following the intragastric administration of the appropriate treatments, rats underwent EZM testing.

2.4.3 | Experiment 3: Prophylactic Treatment

Prophylactic administration was used to further verify the effect of PCC0105004 in the CUMS-induced anxiety model. After 7 days of acclimation to the housing environment, rats were randomly assigned into six groups ($n = 10$ per group): control (Sal) group, vehicle (CUMS + Sal) group, DZP 2 mg/kg group, PCC0105004 (0.5 mg/kg, 1 mg/kg, and 2 mg/kg) groups. During the CUMS period, rats were subjected to various stressors daily for 21 days, except the control group in which rats did not experience the stressors. During the 21 days, rats received intragastric administration twice daily at 8 a.m. and 8 p.m. All rats underwent the battery of behavioral tests beginning on Day 29. At the completion of the behavioral tests, rats from the control, vehicle, and PCC0105004 1 mg/kg groups were euthanized, and the brain tissues were extracted and used for Golgi-Cox staining, RNA-seq analysis, RT-qPCR, and Western blotting analyses.

2.4.4 | Experiment 4: Therapeutic Treatment

Considering the effect of prophylactic administration, we conducted a single therapeutic administration to explore the effect of PCC0105004 in the CUMS-induced anxiety model. After 7 days of acclimation to the housing environment, rats entered the 21-day CUMS period during which they were subjected to various stressors daily except for the control rats ($n = 12$) who did not experience the CUMS. Thereafter, rats were divided into five groups ($n = 12$ per group) for subsequent studies. On Day 29 and thereafter, all rats received their respective acute single treatments (Sal, 2 mg/kg DZP, 0.5 mg/kg, 1 mg/kg, or 2 mg/kg PCC0105004 treatment) and the battery of behavioral tests was performed 30 min after the treatments.

2.5 | Open Field Test

For OFT analyses, a 60 × 60 × 50 cm (length × width × height) box separated into 16 squares of equal size was utilized, defining the central zone as the four central squares. During OFT testing, rats were allowed to explore this box for 5 min, and the TopScan monitoring system (CleverSys Inc. Reston, VA, USA) was used to record their locomotor activity throughout this period. Both total distance traveled and time spent in the central region were recorded.

2.6 | Elevated Zero Maze Test

EZM testing was performed with a black circular track (diameter: 100 cm, width: 10 cm) placed 70 cm above the ground, with two closed and two open runways. Rats were placed within one of the closed arms while facing the open arm, and the amount of time spent in the open arms as well as the number of entrances over a 5-min interval were recorded using the TopScan monitoring system. To prevent any differences in performance among rats, after each animal, the maze was wiped with 75% alcohol spray to remove the trace of the earlier animal.

2.7 | Western Blotting

The brain tissues were sampled from the sacrificed rat immediately after the behavioral tests were carried out. Using the radioimmunoprecipitation assay buffer augmented with enzyme inhibitors, the amygdala was lysed on ice. The tissues were immediately homogenized for western blotting using the primary antibodies stated below: rabbit anti-DCN (1:000, ImmunoWay, Beijing, China, Cat# YN2155), rabbit anti-Ewsr1 (1:1000, ImmunoWay, Cat# YT1645), rabbit anti-Col1a1 (1:1000, ImmunoWay, Cat# YM4807), rabbit anti-Col3a1 (1:1000, abmart, Cat# P02461), mouse anti-GAPDH (1:1000, Beyotime, Shanghai, China, Cat# AF0006), and mouse anti-β-actin (1:1000, Beyotime, Shanghai, China, Cat#AF0003) at 4°C. After washing thrice with TBST and incubating with goat anti-mouse HRP (1:5000, Beyotime, Cat# A0216) and goat anti-rabbit HRP (1:5000, Beyotime, Cat# A0208) for 1 h, ChampChemi 610 (Sagecreation, Beijing, China) was used for protein band detection with imaging being performed with the Sage CapturePro software (Sagecreation, Beijing, China). ImageJ was used to quantify band intensity, normalizing to GAPDH and β-actin.

2.8 | Golgi Staining

The FD Rapid Golgi Stain kit (FD Neuro Technologies) was utilized for brain sample preparation, per the kit's protocol. 150-μm thick coronal sections were sliced via a Leica freezing microtome, inoculated in FD Solution C droplets on gelatin-laminated slides (FD NeuroTechnologies, P0101), mounted, dried overnight at ambient temperature, immersed in the working solution, and then, by using absolute ethanol at 50%, 75%, and 95% concentration, the sections were dehydrated. A microscope (ZEISS, Germany) was then used to view prepared amygdala sections, with the number of spines per 10 μm on a 40-μm dendrite segment being counted for amygdala neurons. Brain tissue sections were prepared from five rats in each group, with quantification having been performed for five neurons per section.

2.9 | RNA-Seq and Data Analysis

High-throughput RNA-seq was performed by Novogene Co. Ltd. (Novogene, Shanghai, China). Briefly, after extracting total RNA from the amygdala samples from rats in the control, model, and drug treatment groups ($n = 3$/group), total RNA was fragmented to generate short segments, and oligo (dT) magnetic beads were used to enrich mRNA, after which cDNA was synthesized. After purifying and enriching the double-stranded cDNA via PCR, BGIseq-500 was used to sequence the library products. KEGG and GO bioinformatics analyses were performed by Novogene with a custom in-house data mining system, and protein–protein interaction (PPI) networks were generated with the STRING database and Cytoscape.

2.10 | RNA Isolation and RT-qPCR

After extracting RNA with an RNA extraction kit, a reverse transcription kit was used to prepare cDNA, and the SYBR Green method was then used for qPCR-based quantification using primer OligodT as directed (Sangong, Shanghai, China). Primers for this study are listed in Table 1. Each 10 μL reaction consisted of 5 μL of 2×SYBR Green qPCR Mix, 0.4 μL each of F + R primers (10 nM), 0.5 μL of prepared cDNA, 0.2 μL of ROX Reference Dye II, and 3.9 μL of RNase Free H_2O. Power SYBR Green PCR Master Mix (Applied Biosystems, CA, USA) and a Fast 7500 Real-Time PCR System (Applied Biosystems) were used for qPCR quantification with the settings: 95°C for 10 min; 40 cycles of 95°C for 15 s and 60°C for 60 s; followed by 95°C for 15 s, 95°C for 60 s, and 95°C for 30 s, and cooling for 30 s at 37°C. Sample gene expression levels were normalized to GAPDH, and the $2^{-\Delta\Delta Ct}$ method was used to quantify relative expression levels among groups.

2.11 | Statistical Analyses

Data are given as means ± SEM. Data were analyzed with IBM SPSS 21.0 (IL, USA) and were graphed with GraphPad Prism 9.0 (CA, USA). Results were compared via one-way ANOVAs with Dunnett's post hoc test, and $p < 0.05$ was considered significant.

2.12 | Nomenclature of Targets and Ligands

Key protein targets and ligands in this article are hyperlinked to corresponding entries in http://www.guidetopharmacology.org, the common portal for data from the IUPHAR/BPS Guide to PHARMACOLOGY [42], and are permanently archived in the Concise Guide to PHARMACOLOGY 2023/24: G protein-coupled receptors [43].

3 | Results

3.1 | Evaluation of the Impact of PCC0105004 on Rat Locomotor Activity and EZM Test

Open field test was used to evaluate the effect of PCC0105004 (1–5 mg/kg, ig) on the spontaneous activity of normal rats. It was shown that PCC0105004 at 1 mg/kg and 2 mg/kg did not have a significant effect on the spontaneous activity of rats. However, higher doses than 3 mg/kg (distance traveled: $p < 0.01$; number of crossings: $p < 0.05$) of PCC0105004 led to significant suppression of the spontaneous activity in rats (Figure 2A,B). To establish the optimal PCC0105004 doses to use in subsequent anxiety-focused studies, the impact of PCC0105004 on anxiety-like behaviors was initially evaluated in normal rats (untreated rats) through the use of the EZM test, which is commonly used to screen for compounds with anxiolytic-like activity when working with rodents [8]. PCC0105004 treatment in the 0.75–2 mg/kg range dose-dependently increased the time the rats spent in the open arms ($p < 0.01$; $p < 0.001$; $p < 0.001$; $p < 0.001$) (Figure 2C) without any impact on the number of entries (Figure 2D). Based on these findings and the OFT results, PCC0105004 doses of 0.5, 1, and 2 mg/kg were selected for further use.

3.2 | Assessment of the Effects of PCC0105004 on Anxiety-Like Behaviors in CUMS Model Rats

A scheme showing the timeline of CUMS treatment and behavioral tests is shown in Figure 3A. After CUMS treatment, rats were subjected to the OFT and EZM tests to evaluate their anxiety-like behaviors. Figure 3F shows the representative tracks of rats in each group during the EZM. As compared to the control

TABLE 1 | Primers for PCR.

Gene	Forward (5′-3′)	Reverse (5′-3′)
Sgk1	CAGAAAAGGAGCGAGTCCGT	GTGAGGGGTTGGCGTTCATA
Aox4	CCCCTTGAATAGCCCAGCAA	AGGGTCGTCTCTGGGAATCA
Col1a1	TGGTACATCAGCCCAAACCC	GCTACGCTGTTCTTGCAGTG
Col3a1	TCAAAGGCCCAGCTGGTATC	TTGCGTCCATCAAAGCCTCT
DCN	GCATGACTTCTGCCTCCCTT	CAATACCGGACAGGGTTGCT
Car13	ATACGACGAGCACAACGGTC	CCACGCAGAACTGATTTGTCC
Nid1	AACCTGGCTATCAGGGGGAT	TCTCGTTCCAGTTGACACCG
Ewsr1	GCAGGGCTACAGTGCTTACA	CAGTGGGAGGCTGTCCATAA
GAPDH	GGTCGGAGTCAACGGATTTG	ATGAGCCCCAGCCTTCTCCAT

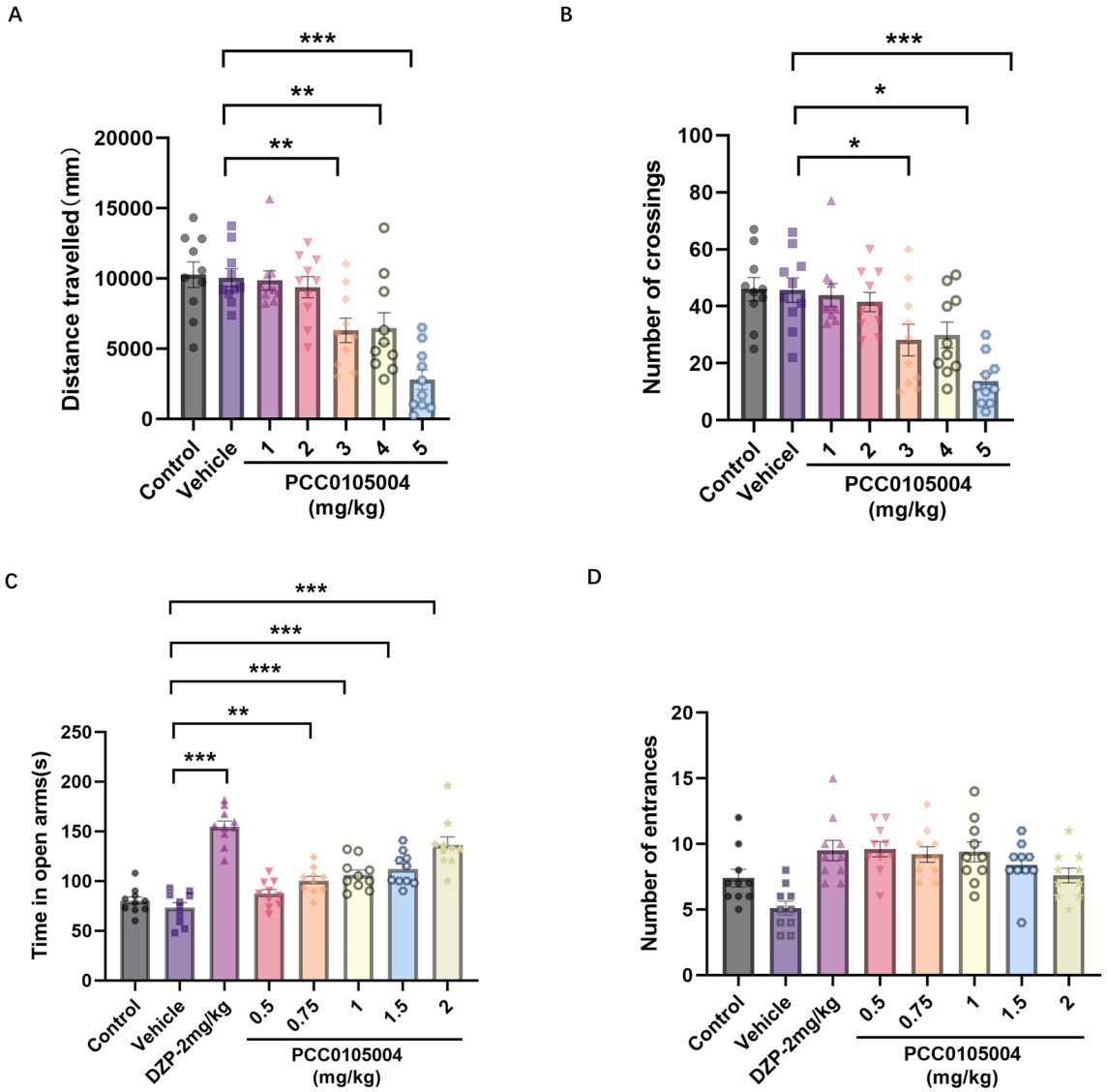

FIGURE 2 | The impact of PCC0105004 on rat locomotion and EZM test performance. OFT numbers of crossings (A) and total distance traveled (B) were analyzed. EZM time in open arms (C) and numbers of entrances (D) were recorded. Data are means ± SEM, $n = 10$/group. One-way ANOVAs with Dunnett's post hoc test, *$p < 0.05$, ** $p < 0.01$, ***$p < 0.001$ vs. vehicle.

rats, the vehicle-treated CUMS model rats spent less time in the open arms ($p < 0.001$) during the EZM test. 21 days of prophylactic treatment with PCC0105004 (0.5, 1 and 2 mg/kg) dose-dependently prevented CUMS-induced anxiety-like behavior in the EZM test ((Figure 3B, $p < 0.05$; $p < 0.001$; $p < 0.001$, respectively) with 2 mg/kg PCC0105004 demonstrating a similar effect to 2 mg/kg DZP $p < 0.001$) treatment. Importantly, the number of entries was not altered by these drug treatments (Figure 3C), demonstrating behavioral specificity. For the OFT, Figure 3G shows the movement trajectories of rats with different treatment histories. As compared to the CUMS model rats with vehicle treatment, PCC0105004 (0.5, 1, and 2 mg/kg) treatment increased the time rats spent in the center of the open field arena (Figure 3D, $p < 0.05$; $p < 0.05$; $p < 0.001$), similar to rats treated with 2 mg/kg DZP ($p < 0.001$). In contrast, no significant effect was found on the total distance traveled in any group of rats (Figure 3E). These results suggest that PCC0105004 treatment was associated with reduced anxiety-like behaviors in CUMS rats while the general locomotor activity of these rats was unaffected.

Next, we examined the acute therapeutic effects of PCC0105004 on CUMS-induced anxiety-like behaviors, wherein a single drug or vehicle treatment was administered 30 min before the behavioral tests (see Figure 4A for study timeline). Figure 4F shows the representative tracks of rats during the EZM. In the EZM test, rats in the vehicle group spent less time in the open arms than those in the control group (Figure 4B, $p < 0.001$), which was dose-dependently and significantly improved by PCC0105004 (1 and 2 mg/kg) ($p < 0.05$; $p < 0.001$) and DZP 2 mg/kg ($p < 0.001$) treatments. The effect was not due to the drugs' impact on the number of entries (Figure 4C). Figure 4G shows the movement trajectories of rats during the OFT. Rats in the vehicle group spent less time in the center arena than those in the control group during the OFT ($p < 0.001$), and PCC0105004 (1 mg/kg and 2 mg/kg) treatment significantly enhanced the time the rats spent in the center arena (Figure 4D, $p < 0.01$; $p < 0.001$) with 2 mg/kg PCC0105004 demonstrating a similar effect to 2 mg/kg DZP ($p < 0.001$). The total distance traveled was not significantly different among the groups (Figure 4E). Together, these results

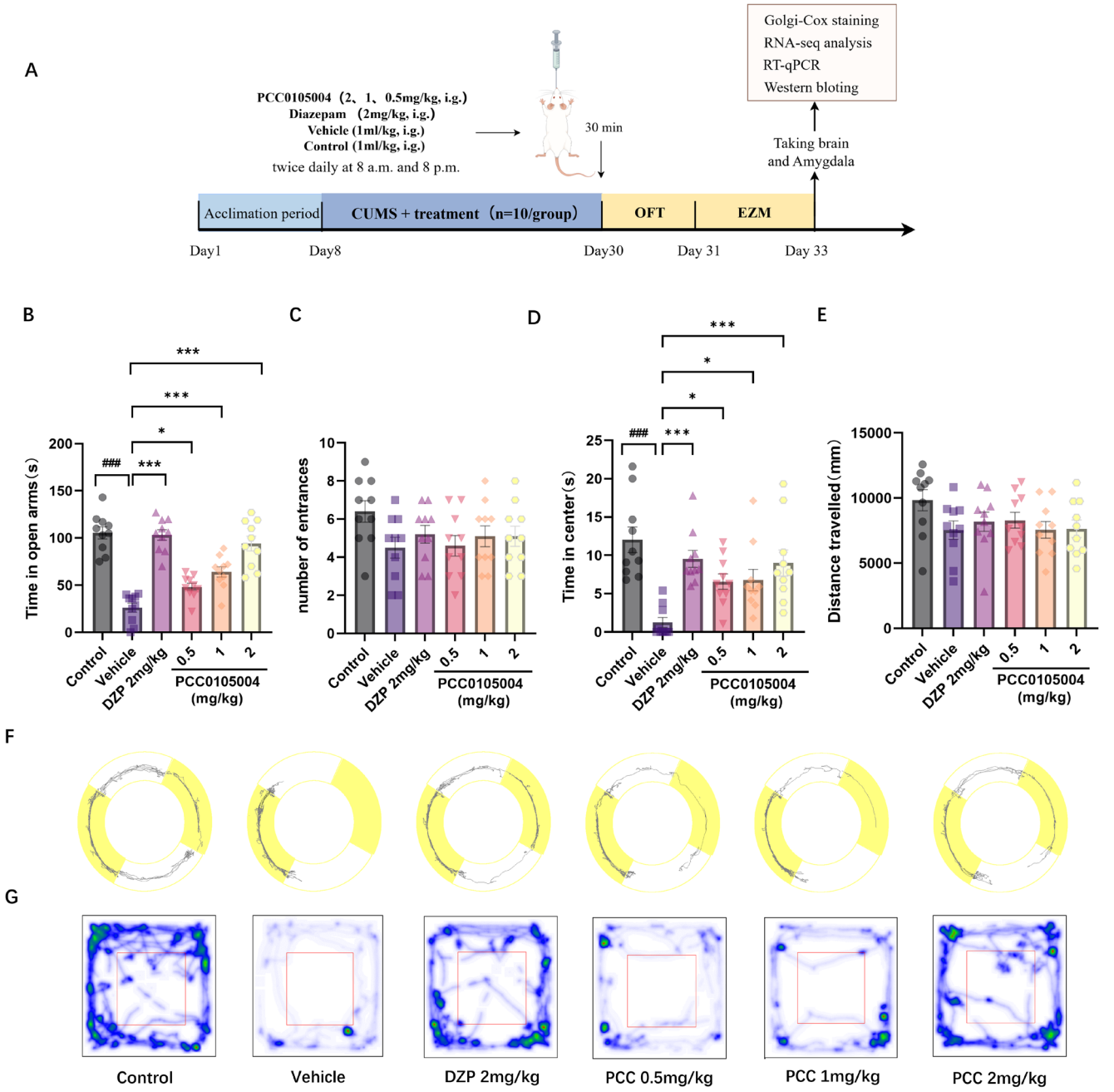

FIGURE 3 | PCC0105004 prophylactically prevents anxiety-like behavior development in CUMS rats. (A) Timeline of prophylactic administration. (B, C) EZM time in open arms (B) and numbers of entrances (C). (D–F) OFT time in center (D) and total distance traveled (E). Typical tracks of the EZM of rats in each group (F). Representative images of the OFT of rats in each group (G). Data are means ± SEM, $n = 10$/group. One-way ANOVAs with Dunnett's post hoc test, ###$p < 0.001$ vs. control, *$p < 0.05$ and ***$p < 0.001$ vs. vehicle.

indicated that PCC0105004 attenuated anxiety-like behaviors in CUMS rats without affecting their locomotor activity.

3.3 | PCC0105004 Reduces Amygdala Dendritic Spine Density

Much evidence suggests that synaptic plasticity dysfunction is involved in the neuropathology of many neuropsychiatric disorders including anxiety disorder [44]. Numbers of literatures have shown that anxiety is closely related to pyramidal neurons [31, 45–47]. Therefore, Golgi staining was next employed to detect changes in dendritic spine morphology in the pyramidal neurons of the amygdala in CUMS rats. Relative to control animals, significantly decreased numbers of total dendritic spines were observed in CUMS model rats ($p < 0.001$), while repeated treatment with 1 mg/kg PCC0105004 during the CUMS period was sufficient to reverse this change (Figure 5, $p < 0.001$), supporting the ability of PCC0105004 to alleviate CUMS-induced synaptic remodeling.

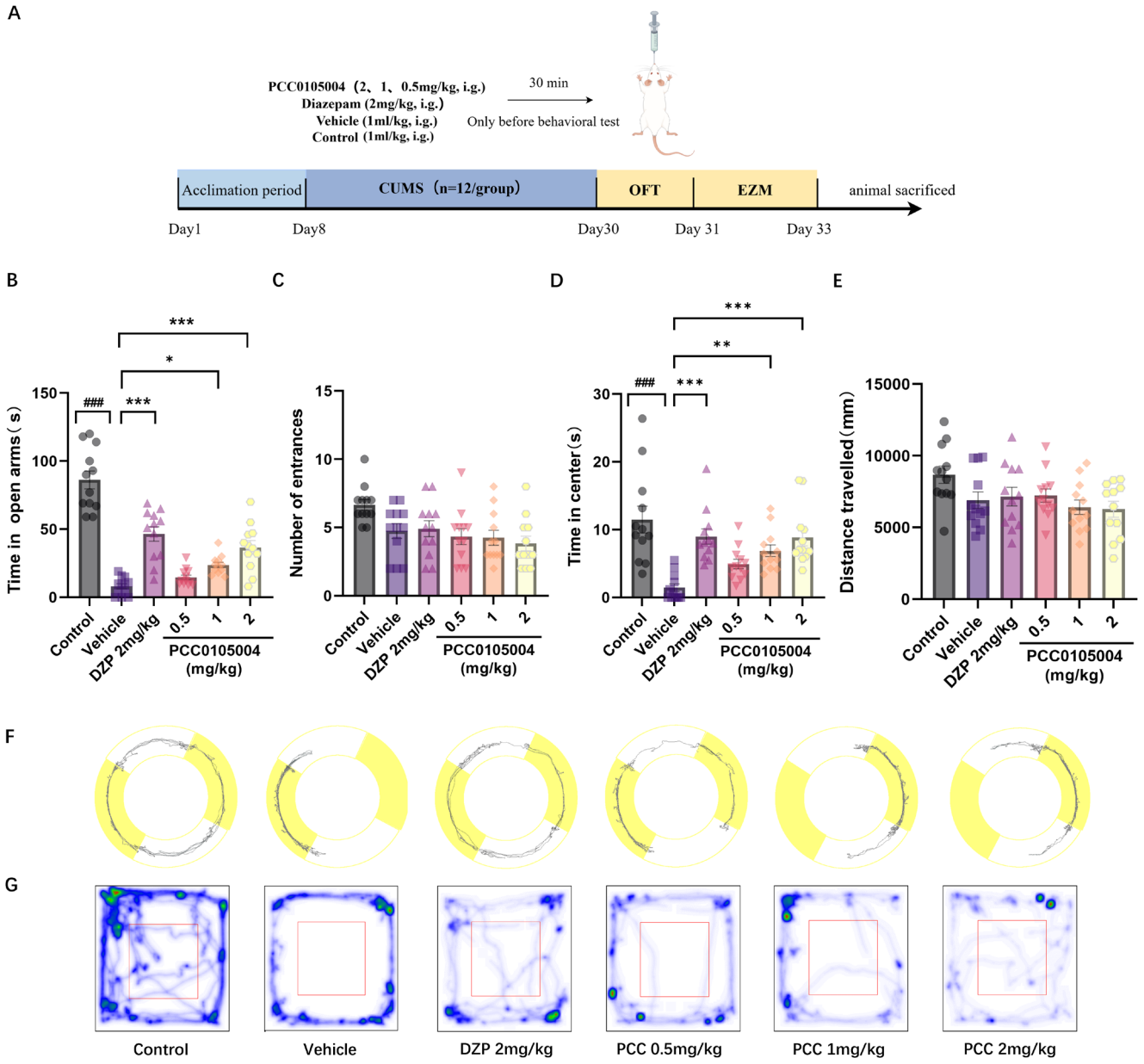

FIGURE 4 | PCC0105004 offers therapeutic protection against anxiety-like behaviors in CUMS model rats. (A) Timeline of therapeutic administration. (B, C) EZM time in open arms (B) and numbers of entrances (C). (D–F) OFT time in center (D) and total distance traveled (E). Typical tracks of the EZM of rats in each group (F). Representative images of the OFT of rats in each group (G). Data are means ± SEM, $n = 10$/group. One-way ANOVAs with Dunnett's post hoc test, ###$p < 0.001$ vs. control, *$p < 0.05$, **$p < 0.01$, and ***$p < 0.001$ vs. vehicle.

3.4 | RNA-Seq Analyses of Amygdala Samples From PCC0105004-Treated Rats

3.4.1 | Correlation Analyses of the Association Between PCC0105004 Treatment and CUMS-Induced Anxiety

The mechanistic basis for the therapeutic benefits of PCC0105004 in CUMS model rats was next assessed through RNA-seq analyses of samples of amygdala tissue from CUMS model rats. In total, 172 and 253 respective upregulated and downregulated genes were detected for the control vs. vehicle comparison, whereas 740 and 195 respective upregulated and downregulated genes were detected when comparing the vehicle and 1 mg/kg PCC0105004 treatment groups (Figure 6A). Clear differences were observed among groups in heatmaps showing the clustering of transcripts in the amygdala (Figure 6C). In total, 93 common anxiety-related genes were identified, accounting for 6.8% of total genes. Overlapping targets were used to establish a PPI network with the STRING database (Figure 6B). This network consisted of 73 and 247 edges, which were significantly higher than the expected 158 edges. Average node degree and local clustering coefficient values were 6.77 and 0.401, while the p value for PPI enrichment was < 3.93e-16, consistent with this network including more than the expected number of interactions. Together, these results indicated the extensive interactions among these proteins and their tightly linked nature. The top 10 core targets from this PPI network included DCN, Col1a1, Col3a1, Col6a2, Nid1, Grm8, Grm2, Cldn2, Actg2, and Cldn1,

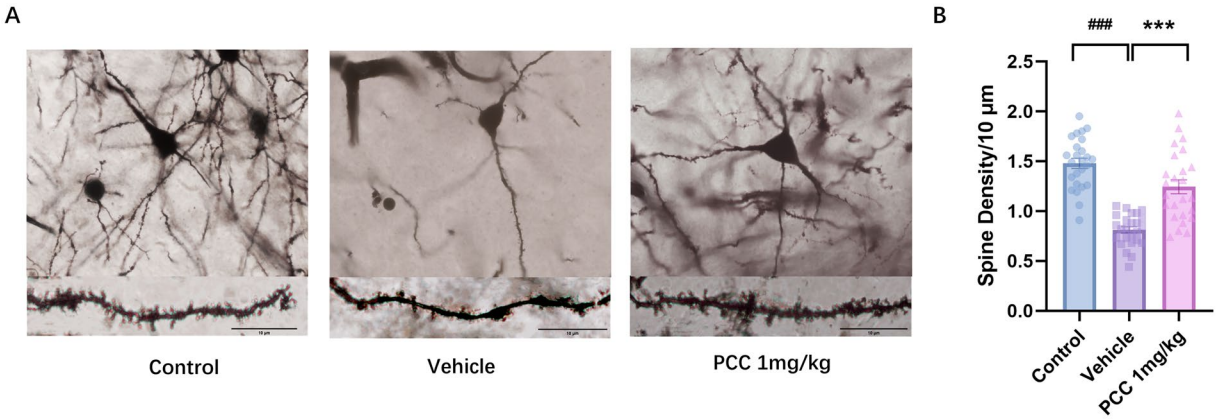

FIGURE 5 | PCC0105004 increases the amygdala dendritic spine density. (A) Representative images of Golgi-stained amygdala pyramidal neurons in rats from the indicated groups. Scale bar: 10 μM. (B) Histograms presenting the numbers of dendritic spines per 10 μm of dendrite length for the amygdala. Data are means ± SEM, $n = 25$/group. One-way ANOVAs with Dunnett's post hoc test, $^{###}p < 0.001$ vs. control, $^{***}p < 0.001$ vs. vehicle.

suggesting the ability of PCC0105004 to exert its anxiolytic effects through signaling pathways related to these targets.

3.4.2 | Functional Enrichment Analyses

To more fully understand the possible functional roles of the identified target genes, the topGO algorithm was next used to perform enrichment analyses. In GO enrichment analyses (Figure 7A), these genes were associated with biological processes including Wnt signaling, transmembrane transport, and cell surface receptor signaling. They were also associated with cellular components including extracellular region and cytoskeleton, and with molecular functions including activity of extracellular matrix structural constituent, calcium ion binding, and transporter activity, suggesting a link between PCC0105004 and these processes.

KEGG pathway enrichment analyses revealed that there were 281 pathways enriched in the PCC0105004 treatment and vehicle treatment groups. Of these pathways, the top 20 were chosen for further analysis (Figure 7B). These pathways revealed the close association between these genes and the regulation of phosphatidylinositol-3-kinase (PI3K)-protein kinase B (AKT) signaling and extracellular matrix (ECM)-receptor interaction pathways, the latter of which is summarized in Figure 7D, and the former of which is summarized in Figure 7E. PCC0105004 was primarily predicted to impact receptors including GPCR, receptor tyrosine kinases, and the ECM, further downregulating downstream factors that include protein kinase C (PKC), serum- and glucocorticoid-inducible kinases (SGK), and cAMP-response element binding protein (CREB). These signaling proteins eventually have effects on cellular events that include survival, growth, and proliferative activity. As shown in Figure 7C, genes and signaling pathways related to PCC0105004 were closely linked, with integrins (including Itgb1, Itgb4, Itgb8, Itga1, Itga5, and Itgav), collagens (including Col1a1, Col4a5, Col6a1, and Col6a2), and laminins (including Lamc1, Lamc3, and Lamc4) serving as key genes. PCC0105004 may thus be capable of mediating anxiolytic effects through its interactions with integrins, collagens, and laminins.

3.5 | Analyses of DEGs Expression and Proteins Related to Synaptic Plasticity in the Amygdala

Next, 88 genes exhibiting opposing trends in the control versus vehicle and vehicle versus PCC0105004 comparisons were analyzed in greater detail. These genes included 23 and 65 that were, respectively, upregulated and downregulated in the control versus vehicle comparison, while exhibiting the opposite expression patterns in the vehicle versus PCC0105004 comparison. In total, these genes included 35 DEGs ($|\log2FC| > 2$, $p < 0.05$, Table 2). Based on the core targets from the PPI network and KEGG pathway enrichment analyses, one upregulated and seven downregulated DEGs from the control versus vehicle comparison were further analyzed (Figure 8A). These analyses revealed the significant upregulation of Ewsr1 (Figure 8H, $p < 0.001$), together with the significant downregulation of *Col1a1*, *Col3a1*, Aox4, *DCN*, and *Car13* (Figure 8B,C,F,G,I *Col1a1*: $p < 0.01$; *Col3a1*: $p < 0.01$; Aox4: $p < 0.001$; DCN: $p < 0.05$; Car13: $p < 0.001$) in vehicle model animals relative to controls. Following repeated treatment with 1 mg/kg PCC0105004 treatment, significantly reduced Ewsr1 expression was observed ($p < 0.001$), while Col1a1, Col3a1, Aox4, and *DCN* were significantly upregulated (Col1a1: $p < 0.001$; Col3a1: $p < 0.01$; Aox4: $p < 0.001$; *DCN*: $p < 0.001$). No corresponding patterns of altered expression were observed for the two remaining DEGs (Figure 8C–E). In light of the above qPCR results, four DEGs associated with synaptic plasticity were selected for further analysis, including *DCN*, *Col1a1*, *Ewsr1*, and *Col3a1*. Western immunoblotting was used to detect the levels of these four proteins, revealing a reduction in *DCN* levels (Figure 8F, $p < 0.001$) and increased Col1a1 and Ewrs1 levels (*Col1a1*: $p < 0.01$; *Ewrs1*: $p < 0.05$) when comparing the control and vehicle groups (Figure 8G,H), while these changes were reversed in PCC0105004-treated rats (*DCN*: $p < 0.01$; *Col1a1*: $p < 0.01$; *Ewsr1*: $p < 0.05$). The Col3a1 protein expression profile did not meet experimental expectations.

4 | Discussion

AD affects millions and currently available therapies suffer from limited efficacy, slow onset, and a myriad of side effects. New

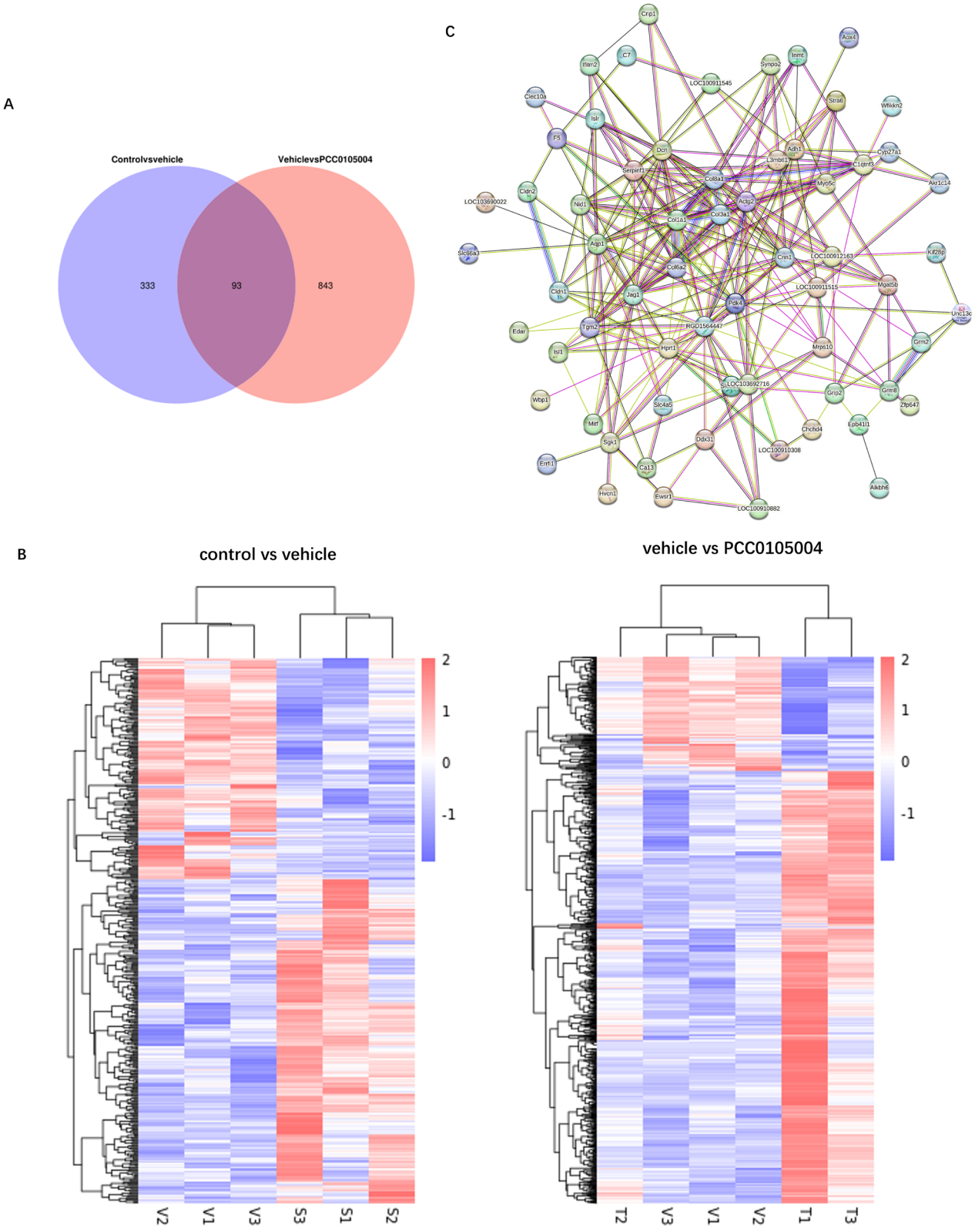

FIGURE 6 | Analyses of correlations between PCC0105004 treatment and CUMS-induced anxiety. (A) Venn diagrams showing overlapping gene expression changes. (B) Heatmaps showing differential gene expression in the control, vehicle, and PCC0105004-treated groups (|Fold-change| > 0, $p < 0.05$). (C) Common target links within a protein–protein interaction network.

anxiolytics with better therapeutic profiles are needed. In this report, we examined the potential anxiolytic effects of a novel TAAR1 agonist PCC0105004 and also examined its underlying anxiolytic mechanisms. In the EZM test, acute PCC0105004 increased the time rats spent in the open arms without affecting the number of entries. In the CUMS model, PCC0105004 was able to prevent and improve anxiety-like behaviors in rats. Morphologically, PCC0105004 prevented CUMS-induced

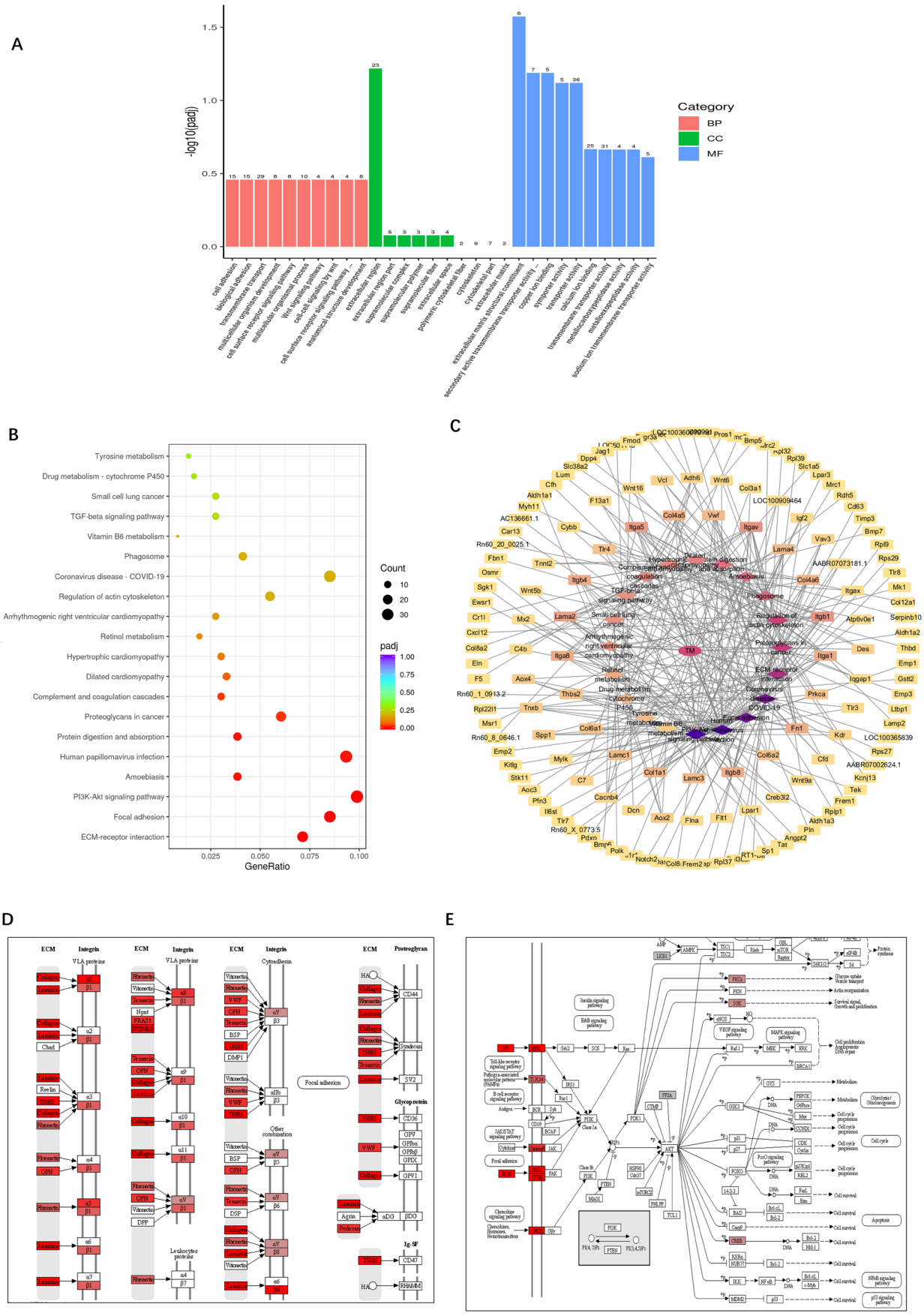

FIGURE 7 | Legend on next page.

FIGURE 7 | Functional enrichment analyses. GO (A) and KEGG (B) enrichment analyses of the genes from the vehicle and PCC0105004 treatment groups. (C) The ECM-receptor interaction and (D) AKT-PI3K signaling pathways and PCC0105004 targets associated with its anxiolytic efficacy. (E) Signaling pathways and targets of PCC0105004 related to its anxiolytic activity. BP, biological processes; CC, cellular components; MF, molecular functions.

synaptic remodeling in the amygdala in rats. At the molecular level, PCC0105004 ameliorated CUMS-induced synaptic changes possibly involving *DCN, Col1a1*, and *Ewsr1* proteins. Together, these results suggest that PCC0105004 has the potential as a novel anxiolytic drug that warrants further examination. A schematic figure depicting the potential mechanisms is shown in Figure 9.

CUMS is a commonly used chronic stress approach, which leads to a behavioral phenotype that is often interpreted and used as rodent behavioral models of several mental disorders including depression and anxiety [48, 49]. When CUMS is used as an experimental manipulation to induce anxiety-like behaviors, behavioral assays such as EZM and OFT are usually used to detect the level of anxiety [50]. EZM was first developed by Shepherd et al. in 1994, which is considered an improvement from the elevated plus maze assay to study anxiety and screen anxiolytic agents [51].

In this study, PCC0105004 significantly increased the time rats spent in the open arms in normal rats and rats that experienced the CUMS protocol, an indicator that is conventionally interpreted as anxiolytic [52, 53]. Because the same doses of PCC0105004 did not affect the number of entries rats crossed the arms, this effect is considered behaviorally specific. Another commonly used anxiolytic assay, OFT [54], was used to replicate the EZM test results with the same rats, and the results were consistent, whereas the rats traveled significantly more in the central arena after PCC0105004 treatment while the total travel distance was unaltered. This indicator also suggests anxiolytic activities [55, 56]. Together, these results strongly suggest that PCC0105004 has anxiolytic activity in rats. Remarkably, SSRIs suffer from a slow onset of therapeutic effect (2–3 weeks) [57], while PPC0105004 shows the effect of anti-anxiety in 24 h. In addition, studies have shown that most patients with acute anxiety symptoms can be treated effectively with benzodiazepines (such as diazepam) [58], but due to tolerance and dependence, benzodiazepines are often restricted. DA transmission is the key monoamine involved in the rewarding and reinforcing effects of almost all addictive drugs [59]. Addictive drugs can increase the concentration of DA in the mesencephalic limbic system of rats [60]. Previous studies showed that TAAR1 was able to negatively modulate dopamine release both in vitro and in vivo [19, 61] and can also specifically inhibit the rewarding and reinforcing effects of drugs of abuse [61]. Thus, PCC0105004 may have a low risk of dependence and deserves further study.

In an effort to more fully explore the anxiolytic activity of PCC0105004 beyond its direct agonistic effects on the TAAR1 receptor, its impact on CUMS-induced synaptic plasticity was evaluated. The amygdala is a key brain region linked to anxiety that undergoes structural plasticity in response to stress [46, 62–64]. The pathogenesis of anxiety is strongly related to synaptic plasticity [65–67]. Recent research suggests that the anxiolytic properties might be mediated by increased dendritic spine density of pyramidal neurons [68], including CUMS-induced anxiety-like behavior and reduced dendritic spine density in the amygdala, which can be partially reversed by the treatment of fragment C of immunoglobulin [69]. In this study, CUMS modeling led to pronounced reductions in dendritic spine density in the amygdala, while PCC0105004 was sufficient to prevent this change. This result probably is not surprising given that the literature suggests that chronic administration of TAAR1 agonists such as RO5263397 can ameliorate chronic stress-induced changes in the structural plasticity of pyramidal neurons [23]. PCC0105004 may therefore be capable of preventing damaging synaptic plasticity maladaptation and reducing the onset and exhibition of anxiety-like behaviors.

Global RNA-seq analyses can provide insight into the signaling pathways and mechanisms related to the incidence of anxiety-related disorders [70, 71]. Combined PPI network, KEGG pathway analysis, and more strictly fold change, when compared with the control group, one upregulated DEGs and seven downregulated DEGs were identified with RT-qPCR in CUMS rats. In particular, PCC0105004 treatment resulted in a significant decrease in mRNA levels of Ewsr1, but gene expressions of Col1a1, Col3a1, Aox4, and DCN were significantly increased. Interestingly, these four DEGs (Ewsr1, Col1a1, Col3a1, and DCN) are known to be associated with synaptic plasticity. To further confirm these changes, we examined the protein expression levels of these four genes. Except for Col3a1 protein, all the other proteins were significantly changed after PCC0105004 treatment.

Decorin (*DCN*) belongs to the small leucine-rich proteoglycan (SLRP) family and is a proteoglycan known to be involved in regulating cell proliferation, collagen fibril organization, and migration [72]. Increasing evidence indicates that upregulation of DCN can improve synaptic remodeling via participating in ECM assembly [73–76]. Besides, it also can regulate the bioactivities of cell growth factors [77–79], including insulin-like growth factor-I receptor (IGF-IR) which can phosphorylate PI3K/AKT/mammalian target of rapamycin (mTOR) pathway, and the pathway has been shown to promote dendritic spine density and synaptic plasticity [80, 81]. These results indicate that there may be positive feedback between synaptic plasticity and DCN. Collagen I is the fibril that forms collagen, encoded by *Col1a1* and *Col1a2* [82]. Growing evidence suggests that collagens are involved in the development of the CNS, playing important roles in neuronal maturation, neural circuit formation, axon guidance, and synaptogenesis [82–84]. Remarkably, they participate in axon guidance and synaptogenesis [85]. Ewing sarcoma breakpoint region 1 (*Ewsr1*) belongs to the FET family; it has been reported that Ewsr1 deficiency leads to neuronal atrophy, affects the stability of neuronal synapses, and causes abnormal motor function [86, 87]. Ewsr1 may activate Akt [88, 89] which is the main regulator

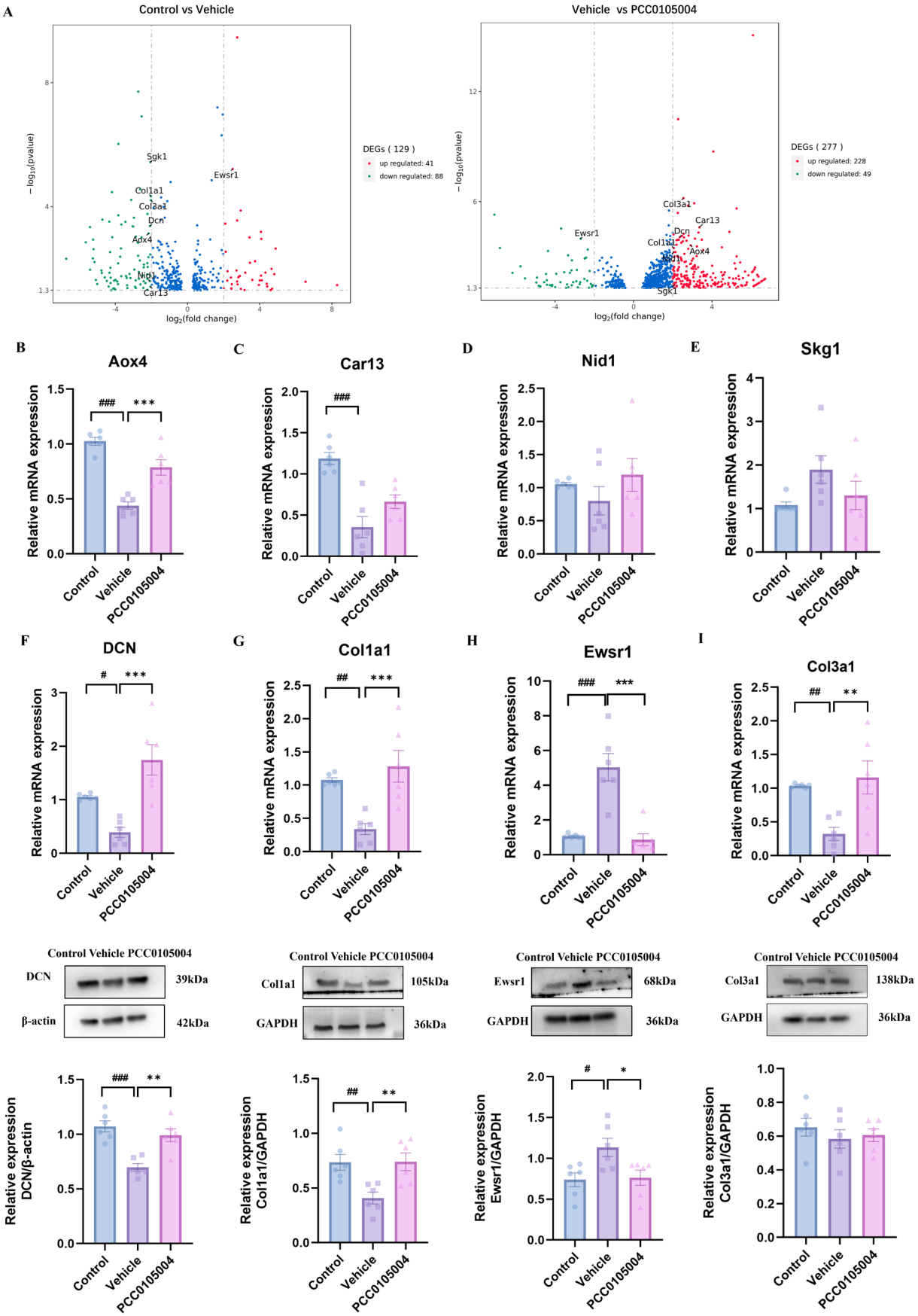

FIGURE 8 | Legend on next page.

FIGURE 8 | Analyses of DEG expression and proteins related to synaptic plasticity in the amygdala. (A) A volcano plot analysis of DEGs in the control, vehicle, and PCC0105004-treated groups (|Fold-change| > 2, $p < 0.05$). (B–E) qPCR analyses of the expression of DEGs including Aox4, Car13, Nidi, and Skg1. (F–I) qPCR and Western blotting analyses of the expression of DEGs and proteins including, DCN, Col1a1, Ewsr1, and Col3a1. Data are means ± SEM, $n = 6$/group. One-way ANOVAs with Dunnett's post hoc test, $^{\#}p < 0.05$, $^{\#\#}p < 0.01$, $^{\#\#\#}p < 0.001$ vs. control, $^{*}p < 0.05$, $^{**}p < 0.01$, and $^{***}p < 0.001$ vs. vehicle.

TABLE 2 | |log2FC| > 2 and p value < 0.05 of the 35 DGEs in transcriptomics.

Gene name	Log2FordChange (Control vs. Vehicle)	Log2FordChange (Vehicle vs. PCC0105004)
Fam111a	6.087783238	−5.209162477
Col3a1	2.545668558	−2.023357244
Car13	3.36043117	−2.052113383
Alkbh6	−3.69210224	2.112584331
LOC100912042	4.884550891	−4.189936608
DCN	2.360253952	−2.080118628
Akr1c14	2.570877151	−2.051191074
Ewsr1	−2.693860324	2.503636249
F5	3.477007554	−3.829764946
Aox4	2.913452023	−2.159200631
Col1a1	2.050079688	−2.036145884
Nid1	2.036764463	−2.090576354
Wbp1	−3.137966902	2.94372669
Slc4a5	2.664696825	−2.550698784
Zfp647	−5.762774416	4.881431847
Aqp1	3.039148016	−2.733072788
LOC100912163	3.046337859	−3.124425256
Lilrb3	−5.531777672	4.652194242
Cnn1	2.833974632	−2.205248763
novel.869	2.740234346	−2.23819329
Cldn2	2.388118623	−2.741084754
Hprt1	−2.717098812	2.198722429
novel.214	−4.953967549	4.070935567
Actg2	3.384609511	−2.694274161
LOC100910308	2.881533171	−2.429210496
Inmt	3.202733973	−3.835407943
Adh6	2.023266851	−3.010001411
Sgk1	2.072070607	−2.054117264
Kif28p	5.322139284	−5.402838666
Chchd4	2.485913138	−2.645112693
Hvcn1	2.264524212	−2.169246441

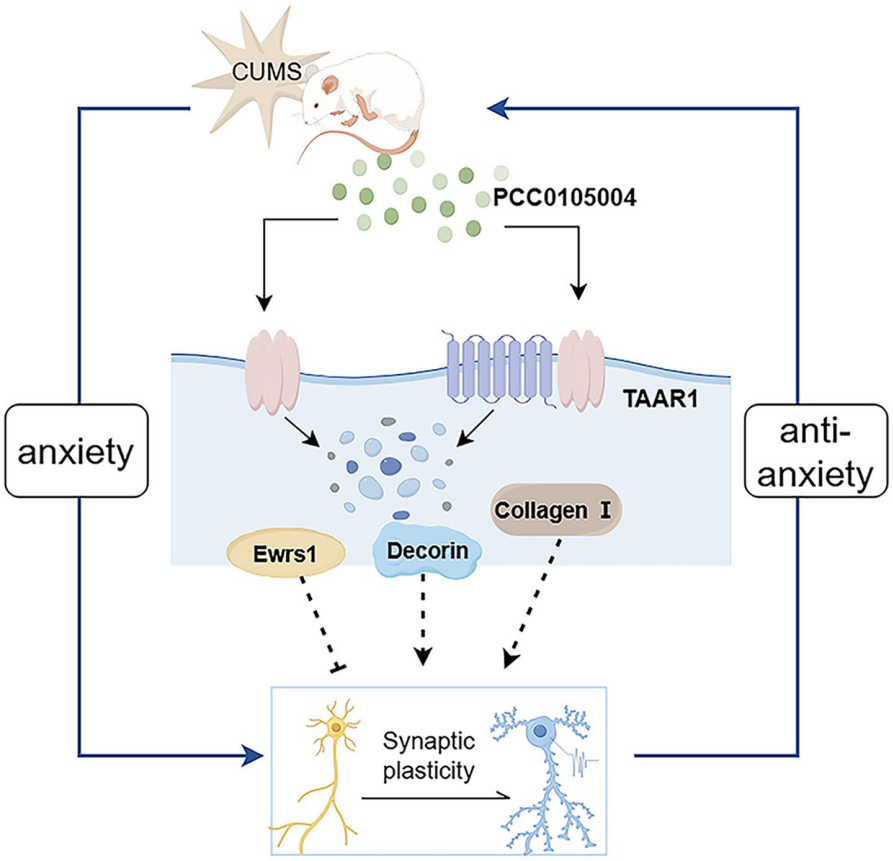

FIGURE 9 | A schematic figure depicts the proposed mechanism of anxiety-behavior modulation by synaptic plasticity.

of cell survival and has key multifunctional downstream signaling nodes, such as glycogen synthase kinase3 (GSK-3) [90]. It has been confirmed that GSK-3 is involved in the regulation of, and cross-talk between, two major forms of synaptic plasticity [91]. In addition, research shows that Ewsr1can regulate the phosphorylation state of CREB [92], which can directly regulate brain-derived neurotrophic factor (BDNF) transcription [93, 94]. It may also be related to its influence on synaptic plasticity. Taken together, the altered protein expressions of these genes in CUMS rats could be directly or indirectly involved in the pathogenesis of CUMS-induced anxiety in rats, and the amelioration of PCC0105004 on these protein changes may contribute to its anxiolytic activity. It should be noted that evidence revealed in this report only suggests their correlative roles, and further investigation is needed to confirm the causal relationships between PCC0105004 treatment, the anxiolytic efficacy, and changes of these synaptic plasticity-related genes.

5 | Conclusion

In summary, the anxiolytic activity of the novel TAAR1 agonist PCC0105004 was herein demonstrated in vivo in rat models of both acute and chronic anxiety, confirming the ability of PCC0105004 to achieve behaviorally specific antianxiety activity. In preliminary studies of the anxiolytic properties of PCC0105004, it was found to attenuate CUMS-induced synaptic remodeling, potentially through the regulation of various genes related to synaptic plasticity such as DCN, Col1a1, and Ewsr1. Combined, these results strongly suggest that the TAAR1 agonist PCC0105004 may be a potentially valuable drug candidate for the treatment of anxiety that is worthy of further investigation.

Author Contributions

Y.Z.: Data curation, Formal analysis, Writing – original draft. L.Y., W.Z.: Investigation, data curation, software. Y.S., M.X.: Conceptualization, Visualization. H.W.: Methodology. C.L.: Methodology, Project administration, Resources, Supervision, Writing – review and editing. J.T.: Funding acquisition, Project administration, Resources.

Acknowledgments

This study was supported by grants from the Science and Technology Project of Yantai (No. 2023XDRH008).

Ethics Statement

The Laboratory Animals Care and Use Committee of Yantai University (Yantai, China) provided approval for all animal studies described herein (registration number: YTU20230110). All measures were taken to ensure minimal discomfort, minimal suffering, and the use of the minimum number of animals possible. The study was conducted in accordance with local legislation and institutional requirements.

Conflicts of Interest

The authors declare no conflicts of interest.

Data Availability Statement

Data pertaining to this article will be available by the corresponding author upon reasonable request.

References

1. M. B. Stein and M. G. Craske, "Treating Anxiety in 2017: Optimizing Care to Improve Outcomes," *JAMA* 318, no. 3 (2017): 235–236.

2. D. J. Stein, K. M. Scott, P. de Jonge, and R. C. Kessler, "Epidemiology of Anxiety Disorders: From Surveys to Nosology and Back," *Dialogues in Clinical Neuroscience* 19, no. 2 (2017): 127–136.

3. A. Baker, N. Simon, A. Keshaviah, et al., "Anxiety Symptoms Questionnaire (ASQ): Development and Validation," *Gen Psychiatr* 32, no. 6 (2019): e100144.

4. A. Garakani, J. W. Murrough, R. C. Freire, et al., "Pharmacotherapy of Anxiety Disorders: Current and Emerging Treatment Options," *Frontiers in Psychiatry* 11 (2020): 595584.

5. M. Shafiee, S. Arekhi, A. Omranzadeh, and A. Sahebkar, "Saffron in the Treatment of Depression, Anxiety and Other Mental Disorders: Current Evidence and Potential Mechanisms of Action," *Journal of Affective Disorders* 227 (2018): 330–337.

6. D. S. Baldwin, A. K. T. Huusom, and E. Mæhlum, "Escitalopram and Paroxetine in the Treatment of Generalised Anxiety Disorder," *British Journal of Psychiatry* 189 (2006): 264–272.

7. T. Sharp and H. Collins, "Mechanisms of SSRI Therapy and Discontinuation," *Current Topics in Behavioral Neurosciences* 66 (2024): 21–47.

8. J. Divljaković, M. Milić, T. Timić, and M. M. Savić, "Tolerance Liability of Diazepam Is Dependent on the Dose Used for Protracted Treatment," *Pharmacological Reports* 64, no. 5 (2012): 1116–1125.

9. C. Cartwright, K. Gibson, J. Read, O. Cowan, and T. Dehar, "Long-Term Antidepressant Use: Patient Perspectives of Benefits and Adverse Effects," *Patient Preference and Adherence* 10 (2016): 1401–1407.

10. D. S. Baldwin, S. Waldman, and C. Allgulander, "Evidence-Based Pharmacological Treatment of Generalized Anxiety Disorder," *International Journal of Neuropsychopharmacology* 14, no. 5 (2011): 697–710.

11. S. D. Liberles and L. B. Buck, "A Second Class of Chemosensory Receptors in the Olfactory Epithelium," *Nature* 442, no. 7103 (2006): 645–650.

12. G. Rutigliano, A. Accorroni, and R. Zucchi, "The Case for TAAR1 as a Modulator of Central Nervous System Function," *Frontiers in Pharmacology* 8 (2017): 987.

13. H. J. Shi, S. Wang, X. P. Wang, R. X. Zhang, and L. J. Zhu, "Hippocampus: Molecular, Cellular, and Circuit Features in Anxiety," *Neuroscience Bulletin* 39, no. 6 (2023): 1009–1026.

14. W. Z. Liu, W. H. Zhang, Z. H. Zheng, et al., "Identification of a Prefrontal Cortex-To-Amygdala Pathway for Chronic Stress-Induced Anxiety," *Nature Communications* 11, no. 1 (2020): 2221.

15. G. Rutigliano, J. Bräunig, C. Del Grande, et al., "Non-Functional Trace Amine-Associated Receptor 1 Variants in Patients With Mental Disorders," *Frontiers in Pharmacology* 10 (2019): 1027.

16. S. M. Underhill, M. S. Colt, and S. G. Amara, "Amphetamine Stimulates Endocytosis of the Norepinephrine and Neuronal Glutamate Transporters in Cultured Locus Coeruleus Neurons," *Neurochemical Research* 45, no. 6 (2020): 1410–1419.

17. I. Sukhanov, S. Espinoza, D. S. Yakovlev, M. C. Hoener, T. D. Sotnikova, and R. R. Gainetdinov, "TAAR1-Dependent Effects of Apomorphine in Mice," *International Journal of Neuropsychopharmacology* 17, no. 10 (2014): 1683–1693.

18. F. G. Revel, J. L. Moreau, R. R. Gainetdinov, et al., "Trace Amine-Associated Receptor 1 Partial Agonism Reveals Novel Paradigm for Neuropsychiatric Therapeutics," *Biological Psychiatry* 72, no. 11 (2012): 934–942.

19. F. G. Revel, J. L. Moreau, R. R. Gainetdinov, et al., "TAAR1 Activation Modulates Monoaminergic Neurotransmission, Preventing Hyperdopaminergic and Hypoglutamatergic Activity," *Proceedings of the National Academy of Sciences of the United States of America* 108, no. 20 (2011): 8485–8490.

20. Y. Alnefeesi, J. K. Tamura, L. M. W. Lui, et al., "Trace Amine-Associated Receptor 1 (TAAR1): Potential Application in Mood Disorders: A Systematic Review," *Neuroscience and Biobehavioral Reviews* 131 (2021): 192–210.

21. N. Dedic, H. Dworak, C. Zeni, G. Rutigliano, and O. D. Howes, "Therapeutic Potential of TAAR1 Agonists in Schizophrenia: Evidence From Preclinical Models and Clinical Studies," *International Journal of Molecular Sciences* 22, no. 24 (2021): 13185.

22. L. Peng, J. Zhang, J. Feng, et al., "Activation of Trace Amine-Associated Receptor 1 Ameliorates PTSD-Like Symptoms," *Biochemical Pharmacology* 228 (2024): 116236.

23. Y. Zhang, J. T. Li, H. Wang, et al., "Role of Trace Amine-Associated Receptor 1 in the Medial Prefrontal Cortex in Chronic Social Stress-Induced Cognitive Deficits in Mice," *Pharmacological Research* 167 (2021): 105571.

24. Y. Alnefeesi, I. Sukhanov, and R. R. Gainetdinov, "Ligands of the Trace Amine-Associated Receptors (TAARs): A New Class of Anxiolytics," *Pharmacology, Biochemistry, and Behavior* 242 (2024): 173817.

25. G. G. Calhoon and K. M. Tye, "Resolving the Neural Circuits of Anxiety," *Nature Neuroscience* 18, no. 10 (2015): 1394–1404.

26. K. M. Tye, R. Prakash, S.-Y. Kim, et al., "Amygdala Circuitry Mediating Reversible and Bidirectional Control of Anxiety," *Nature* 471, no. 7338 (2011): 358–362.

27. Z. H. Zheng, J. L. Tu, X. H. Li, et al., "Neuroinflammation Induces Anxiety- and Depressive-Like Behavior by Modulating Neuronal Plasticity in the Basolateral Amygdala," *Brain, Behavior, and Immunity* 91 (2021): 505–518.

28. J. Y. Zhang, T. H. Liu, Y. He, et al., "Chronic Stress Remodels Synapses in an Amygdala Circuit-Specific Manner," *Biological Psychiatry* 85, no. 3 (2019): 189–201.

29. K. Monsorno, K. Ginggen, A. Ivanov, et al., "Loss of Microglial MCT4 Leads to Defective Synaptic Pruning and Anxiety-Like Behavior in Mice," *Nature Communications* 14, no. 1 (2023): 5749.

30. D. J. Christoffel, S. A. Golden, and S. J. Russo, "Structural and Synaptic Plasticity in Stress-Related Disorders," *Reviews in the Neurosciences* 22, no. 5 (2011): 535–549.

31. Q. Cui, S. Liang, H. Li, et al., "SNX17 Mediates Dendritic Spine Maturation via p140Cap," *Molecular Neurobiology* 61, no. 3 (2024): 1346–1362.

32. D. Chen, Q. Lou, X. J. Song, et al., "Microglia Govern the Extinction of Acute Stress-Induced Anxiety-Like Behaviors in Male Mice," *Nature Communications* 15, no. 1 (2024): 449.

33. B. Wang, T. Zhao, X. X. Chen, et al., "Gestational 1-Nitropyrene Exposure Causes Anxiety-Like Behavior Partially by Altering Hippocampal Epigenetic Reprogramming of Synaptic Plasticity in Male Adult Offspring," *Journal of Hazardous Materials* 453 (2023): 131427.

34. R. Mitra, D. Ferguson, and R. M. Sapolsky, "SK2 Potassium Channel Overexpression in Basolateral Amygdala Reduces Anxiety, Stress-Induced Corticosterone Secretion and Dendritic Arborization," *Molecular Psychiatry* 14, no. 9 (2009): 847–855, 827.

35. F. Xu, L. Han, Y. Wang, et al., "Prolonged Anesthesia Induces Neuroinflammation and Complement-Mediated Microglial Synaptic Elimination Involved in Neurocognitive Dysfunction and Anxiety-Like Behaviors," *BMC Medicine* 21, no. 1 (2023): 7.

36. L. Yu, W. Zhang, Y. Shi, et al., "TAAR1 as a New Target for the Treatment of Bipolar Disorder: Anti-Manic and Anti-Depressant Activity of

the Novel Agonist PCC0105004," *Journal of Pharmaceutical and Biopharmaceutical Research* 5 (2024): 396–411.

37. N. Ogawa, C. Hara, and S. Takaki, "Anxiolytic Activity of SC-48274 Compared With Those of Buspirone and Diazepam in Experimental Anxiety Models," *Japanese Journal of Pharmacology* 61, no. 2 (1993): 115–121.

38. M. P. Dandekar, M. S. K. Palepu, S. Satti, et al., "Multi-Strain Probiotic Formulation Reverses Maternal Separation and Chronic Unpredictable Mild Stress-Generated Anxiety- and Depression-Like Phenotypes by Modulating Gut Microbiome-Brain Activity in Rats," *ACS Chemical Neuroscience* 13, no. 13 (2022): 1948–1965.

39. X. Song, W. Wang, S. Ding, et al., "Exploring the Potential Antidepressant Mechanisms of Puerarin: Anti-Inflammatory Response via the Gut-Brain axis," *Journal of Affective Disorders* 310 (2022): 459–471.

40. S. W. Chen, W. J. Wang, W. J. Li, et al., "Anxiolytic-Like Effect of Asiaticoside in Mice," *Pharmacology, Biochemistry, and Behavior* 85, no. 2 (2006): 339–344.

41. A. R. Colla, J. M. Rosa, M. P. Cunha, and A. L. Rodrigues, "Anxiolytic-Like Effects of Ursolic Acid in Mice," *European Journal of Pharmacology* 758 (2015): 171–176.

42. S. D. Harding, J. L. Sharman, E. Faccenda, et al., "The IUPHAR/BPS Guide to PHARMACOLOGY in 2018: Updates and Expansion to Encompass the New Guide to IMMUNOPHARMACOLOGY," *Nucleic Acids Research* 46, no. D1 (2018): D1091–d1106.

43. S. P. H. Alexander, A. Christopoulos, A. P. Davenport, et al., "The Concise Guide to PHARMACOLOGY 2023/24: G Protein-Coupled Receptors," *British Journal of Pharmacology* 180, no. Suppl 2 (2023): S23–s144.

44. M. He, J. X. Wei, M. Mao, et al., "Synaptic Plasticity in PTSD and Associated Comorbidities: The Function and Mechanism for Diagnostics and Therapy," *Current Pharmaceutical Design* 24, no. 34 (2018): 4051–4059.

45. S. Moreno-Martínez, H. Tendilla-Beltrán, V. Sandoval, G. Flores, and J. A. Terrón, "Chronic Restraint Stress Induces Anxiety-Like Behavior and Remodeling of Dendritic Spines in the Central Nucleus of the Amygdala," *Behavioural Brain Research* 416 (2022): 113523.

46. B. Leuner and T. J. Shors, "Stress, Anxiety, and Dendritic Spines: What Are the Connections?," *Neuroscience* 251 (2013): 108–119.

47. E. Soztutar, E. Colak, and E. Ulupinar, "Gender- and Anxiety Level-Dependent Effects of Perinatal Stress Exposure on Medial Prefrontal Cortex," *Experimental Neurology* 275, no. Pt 2 (2016): 274–284.

48. L. Sun, L. Ma, H. Zhang, et al., "Fto Deficiency Reduces Anxiety- and Depression-Like Behaviors in Mice via Alterations in Gut Microbiota," *Theranostics* 9, no. 3 (2019): 721–733.

49. Q. Fu, R. Qiu, L. Chen, Y. Chen, W. Qi, and Y. Cheng, "Music Prevents Stress-Induced Depression and Anxiety-Like Behavior in Mice," *Translational Psychiatry* 13, no. 1 (2023): 317.

50. K. Małyszczak and M. Szechiński, "Comorbidity of Different Forms of Anxiety Disorders and Depression," *Psychiatria Polska* 38, no. 4 (2004): 603–609.

51. R. Danduga and P. K. Kola, "Elevated Plus Maze for Assessment of Anxiety and Memory in Rodents," *Methods in Molecular Biology* 2761 (2024): 93–96.

52. J. K. Shepherd, S. S. Grewal, A. Fletcher, D. J. Bill, and C. T. Dourish, "Behavioural and Pharmacological Characterisation of the Elevated "Zero-Maze" as an Animal Model of Anxiety," *Psychopharmacology* 116, no. 1 (1994): 56–64.

53. A. A. Walf and C. A. Frye, "The Use of the Elevated Plus Maze as an Assay of Anxiety-Related Behavior in Rodents," *Nature Protocols* 2, no. 2 (2007): 322–328.

54. R. M. Deacon, A. Croucher, and J. N. Rawlins, "Hippocampal Cytotoxic Lesion Effects on Species-Typical Behaviours in Mice," *Behavioural Brain Research* 132, no. 2 (2002): 203–213.

55. E. Ericson, J. Samuelsson, and S. Ahlenius, "Photocell Measurements of Rat Motor Activity. A Contribution to Sensitivity and Variation in Behavioral Observations," *Journal of Pharmacological Methods* 25, no. 2 (1991): 111–122.

56. P. L. Broadhurst, "The Place of Animal Psychology in the Development of Psychosomatic Research," *Fortschritte der Psychosomatischen Medizin* 1 (1960): 63–69.

57. C. J. Harmer, R. S. Duman, and P. J. Cowen, "How Do Antidepressants Work? New Perspectives for Refining Future Treatment Approaches," *Lancet Psychiatry* 4, no. 5 (2017): 409–418.

58. S. Romanazzo, G. Mansueto, and F. Cosci, "Anxiety in the Medically Ill: A Systematic Review of the Literature," *Frontiers in Psychiatry* 13 (2022): 873126.

59. J. Liu, R. Wu, and J. X. Li, "TAAR1 as an Emerging Target for the Treatment of Psychiatric Disorders," *Pharmacology & Therapeutics* 253 (2024): 108580.

60. R. A. Wise and C. J. Jordan, "Dopamine, Behavior, and Addiction," *Journal of Biomedical Science* 28, no. 1 (2021): 83.

61. J. F. Liu and J. X. Li, "TAAR1 in Addiction: Looking Beyond the Tip of the Iceberg," *Frontiers in Pharmacology* 9 (2018): 279.

62. M. Davis, "The Role of the Amygdala in Fear and Anxiety," *Annual Review of Neuroscience* 15 (1992): 353–375.

63. J. E. LeDoux, "Coming to Terms With Fear," *Proceedings of the National Academy of Sciences of the United States of America* 111, no. 8 (2014): 2871–2878.

64. X. D. Yu, Y. Zhu, Q. X. Sun, et al., "Distinct Serotonergic Pathways to the Amygdala Underlie Separate Behavioral Features of Anxiety," *Nature Neuroscience* 25, no. 12 (2022): 1651–1663.

65. K. Hashimoto, "BDNF Variant Linked to Anxiety-Related Behaviors," *BioEssays* 29, no. 2 (2007): 116–119.

66. Y. Cheng, Y. Wang, W. Zhang, J. Yin, J. Dong, and J. Liu, "Relationship Between Intestinal Flora, Inflammation, BDNF Gene Polymorphism and Generalized Anxiety Disorder: A Clinical Investigation," *Medicine (Baltimore)* 101, no. 29 (2022): e28910.

67. H. A. Chang, W. H. Fang, Y. P. Liu, et al., "BDNF $Val^{66}Met$ Polymorphism to Generalized Anxiety Disorder Pathways: Indirect Effects via Attenuated Parasympathetic Stress-Relaxation Reactivity," *Journal of Abnormal Psychology* 129, no. 3 (2020): 237–247.

68. D. De Gregorio, A. Inserra, J. P. Enns, et al., "Repeated Lysergic Acid Diethylamide (LSD) Reverses Stress-Induced Anxiety-Like Behavior, Cortical Synaptogenesis Deficits and Serotonergic Neurotransmission Decline," *Neuropsychopharmacology* 47, no. 6 (2022): 1188–1198.

69. L. Lin, X. F. Zhou, and L. Bobrovskaya, "Blockage of p75(NTR) Ameliorates Depressive-Like Behaviours of Mice Under Chronic Unpredictable Mild Stress," *Behavioural Brain Research* 396 (2021): 112905.

70. L. Zou, Y. Tian, Y. Wang, et al., "High-Cholesterol Diet Promotes Depression- and Anxiety-Like Behaviors in Mice by Impact Gut Microbe and Neuroinflammation," *Journal of Affective Disorders* 327 (2023): 425–438.

71. D. Nikolopoulos, T. Manolakou, A. Polissidis, et al., "Microglia Activation in the Presence of Intact Blood-Brain Barrier and Disruption of Hippocampal Neurogenesis via IL-6 and IL-18 Mediate Early Diffuse Neuropsychiatric Lupus," *Annals of the Rheumatic Diseases* 82, no. 5 (2023): 646–657.

72. A. Kedem, K. Ulanenko-Shenkar, Y. Yung, G. M. Yerushalmi, E. Maman, and A. Hourvitz, "Elucidating Decorin's Role in the Preovulatory Follicle," *Journal of Ovarian Research* 13, no. 1 (2020): 15.

73. W. Zhang, Y. Ge, Q. Cheng, Q. Zhang, L. Fang, and J. Zheng, "Decorin Is a Pivotal Effector in the Extracellular Matrix and Tumour Microenvironment," *Oncotarget* 9, no. 4 (2018): 5480–5491.

74. S. Kanzler, A. W. Lohse, A. Keil, et al., "TGF-beta1 in Liver Fibrosis: An Inducible Transgenic Mouse Model to Study Liver Fibrogenesis," *American Journal of Physiology* 276, no. 4 (1999): G1059–G1068.

75. N. Klapka, S. Hermanns, G. Straten, et al., "Suppression of Fibrous Scarring in Spinal Cord Injury of Rat Promotes Long-Distance Regeneration of Corticospinal Tract Axons, Rescue of Primary Motoneurons in Somatosensory Cortex and Significant Functional Recovery," *European Journal of Neuroscience* 22, no. 12 (2005): 3047–3058.

76. J. R. Harper, R. C. Spiro, W. A. Gaarde, et al., "Role of Transforming Growth Factor beta and Decorin in Controlling Fibrosis," *Methods in Enzymology* 245 (1994): 241–254.

77. L. Schaefer, W. Tsalastra, A. Babelova, et al., "Decorin-Mediated Regulation of Fibrillin-1 in the Kidney Involves the Insulin-Like Growth Factor-I Receptor and Mammalian Target of Rapamycin," *American Journal of Pathology* 170, no. 1 (2007): 301–315.

78. F. Caraci, W. Gulisano, C. A. Guida, et al., "A Key Role for TGF-β1 in Hippocampal Synaptic Plasticity and Memory," *Scientific Reports* 5 (2015): 11252.

79. J. Rong, Y. Yang, M. Liang, et al., "Neonatal Inflammation Increases Hippocampal KCC2 Expression Through Methylation-Mediated TGF-β1 Downregulation Leading to Impaired Hippocampal Cognitive Function and Synaptic Plasticity in Adult Mice," *Journal of Neuroinflammation* 20, no. 1 (2023): 15.

80. Y. Wu, Z. Zhu, T. Lan, et al., "Levomilnacipran Improves Lipopolysaccharide-Induced Dysregulation of Synaptic Plasticity and Depression-Like Behaviors via Activating BDNF/TrkB Mediated PI3K/Akt/mTOR Signaling Pathway," *Molecular Neurobiology* 61, no. 7 (2024): 4102–4115.

81. Q. Yuan, F. J. Wang, Z. Z. Jia, et al., "Xueshuantong Injection Combined With Salvianolate Lyophilized Injection Improves the Synaptic Plasticity Against Focal Cerebral Ischemia/Reperfusion Injury in Rats Through PI3K/AKT/mTOR and RhoA/ROCK Pathways," *Brain Research* 1787 (2022): 147923.

82. T. Hubert, S. Grimal, P. Carroll, and A. Fichard-Carroll, "Collagens in the Developing and Diseased Nervous System," *Cellular and Molecular Life Sciences* 66, no. 7 (2009): 1223–1238.

83. A. L. Sertié, V. Sossi, A. A. Camargo, M. Zatz, C. Brahe, and M. R. Passos-Bueno, "Collagen XVIII, Containing an Endogenous Inhibitor of Angiogenesis and Tumor Growth, Plays a Critical Role in the Maintenance of Retinal Structure and in Neural Tube Closure (Knobloch Syndrome)," *Human Molecular Genetics* 9, no. 13 (2000): 2051–2058.

84. L. K. Wareham, R. O. Baratta, B. J. Del Buono, E. Schlumpf, and D. J. Calkins, "Collagen in the Central Nervous System: Contributions to Neurodegeneration and Promise as a Therapeutic Target," *Molecular Neurodegeneration* 19, no. 1 (2024): 11.

85. M. A. Fox, "Novel Roles for Collagens in Wiring the Vertebrate Nervous System," *Current Opinion in Cell Biology* 20, no. 5 (2008): 508–513.

86. J. W. Jung, H. Kim, J. Park, et al., "In-Depth Proteome Analysis of Brain Tissue From Ewsr1 Knockout Mouse by Multiplexed Isobaric Tandem Mass Tag Labeling," *Scientific Reports* 13, no. 1 (2023): 15261.

87. Y. Yoon, H. Park, S. Kim, et al., "Genetic Ablation of EWS RNA Binding Protein 1 (EWSR1) Leads to Neuroanatomical Changes and Motor Dysfunction in Mice," *Exp Neurobiol* 27, no. 2 (2018): 103–111.

88. P. Svenningsson, A. Nishi, G. Fisone, J. A. Girault, A. C. Nairn, and P. Greengard, "DARPP-32: An Integrator of Neurotransmission," *Annual Review of Pharmacology and Toxicology* 44 (2004): 269–296.

89. A. Avanes, G. Lenz, and J. Momand, "Darpp-32 and t-Darpp Protein Products of PPP1R1B: Old Dogs With New Tricks," *Biochemical Pharmacology* 160 (2019): 71–79.

90. B. Vangamudi, D. F. Peng, Q. Cai, W. El-Rifai, W. Zheng, and A. Belkhiri, "T-DARPP Regulates Phosphatidylinositol-3-Kinase-Dependent Cell Growth in Breast cancer," *Molecular Cancer* 9 (2010): 240.

91. S. Peineau, C. Bradley, C. Taghibiglou, et al., "The Role of GSK-3 in Synaptic Plasticity," *British Journal of Pharmacology* 153, no. 1 (2008): S428–S437.

92. C. Fekete, E. Mihály, S. Herscovici, et al., "DARPP-32 and CREB Are Present in Type 2 Iodothyronine Deiodinase-Producing Tanycytes: Implications for the Regulation of Type 2 Deiodinase Activity," *Brain Research* 862, no. 1–2 (2000): 154–161.

93. X. Ren, H. S. Rizavi, M. A. Khan, R. Bhaumik, Y. Dwivedi, and G. N. Pandey, "Alteration of Cyclic-AMP Response Element Binding Protein in the Postmortem Brain of Subjects With Bipolar Disorder and Schizophrenia," *Journal of Affective Disorders* 152-154 (2014): 326–333.

94. C. S. Wang, E. T. Kavalali, and L. M. Monteggia, "BDNF Signaling in Context: From Synaptic Regulation to Psychiatric Disorders," *Cell* 185, no. 1 (2022): 62–76.